INFLUENCE OF THE WAKE INTERFERENCE ON THE VORTEX SHEDDING FLOW AROUND A CIRCULAR CYLINDER IN GROUND EFFECT

Alex Mendonça Bimbato, alexbimbato@unifei.edu.br
Luiz Antonio Alcântara Pereira, luizantp@unifei.edu.br
Institute of Mechanical Engineering, Federal University of Itajuba, Itajuba, Minas Gerais, Brazil, CP 50

Miguel Hiroo Hirata, hirata@fat.uerj.br
State University of Rio de Janeiro, FAT-UERJ, Resende, Rio de Janeiro, Brazil

Abstract. *The effects of the distance between the circular cylinder and the plane surface are still far from being fully understood due the variety of other influencing factors, in particular the confusing influence of the boundary layer formed on the ground, or "wake interference". A ground moving with the incoming flow velocity, however, does not allow the development of a boundary layer. The vortex shedding flow around a circular cylinder near a plane boundary at high Reynolds number is studied here numerically. A Lagrangian purely vortex method is used in association with an integral formulation derived from a Poisson equation for the pressure to compute the aerodynamic loads acting on the cylinder surface in ground effect. Both situations of fixed ground and moving ground are analyzed. The numerical results are compared with experimental ones available in the literature and show that when using fixed ground, the absolute value of the maximum of the C_D curve is bigger than the absolute value of the maximum of the moving ground C_D curve; the wake interference is the one responsible for a "great" maximum value of the C_D curve.*

Keywords: vortex method, ground effect, wake interference, aerodynamic loads, bluff body

1. INTRODUCTION

The phenomenon of vortex shedding from a two-dimensional bluff body has been studied by various researchers in the past few decades. The viscous flow around a bluff body includes a variety of fluid dynamics phenomena, such as separation, vortex shedding and the transition to turbulence; all these phenomena have practical importance in engineering and scientific relevance in fluid mechanics. Understanding vortex-shedding is of great importance in the design of a variety of offshore engineering structures, tall buildings, bridges, chimneys, heat exchanger tubes and electricity cables. The characteristics of flow around bluff bodies are in general highly complicated, and many experimental and computational efforts are necessary to fully understand it.

In order to understand such general complex flows, it is reasonable to study the flow around bodies of simple geometry. Among them, the circular cylinders are very suitable for restricting the complexity and thus observing the fundamental features of the flow. In fact, the flow around cylinders has been extensively studied not only to understand the fundamentals of general bluff body flows but also because this flow configuration is of direct relevance to many practical applications. It is interesting to mention that the flow around cylinders in experimental studies is direct influenced by the end conditions of the cylinder.

It is well known in the literature that the Kármán vortex shedding generates alternating lift force exerting on the cylinder; in addition it can induce large cross flow oscillation. Since the Kármán vortex excitation is observed when the cylinder is placed near a plane boundary, enormous efforts have been devoted to clarifying its mechanism. The characteristics of flow around a circular cylinder near a ground are governed not only by the Reynolds number, but also by "gap ratio", i.e., the ratio of the gap between the cylinder and the ground boundary to the cylinder diameter, h/d. In experimental work as well in numerical simulations, the fixed ground plane develops a boundary layer that interferes with the body viscous wake, leading to not so precise results.

Roshko *et al.* (1975) measured the time-averaged drag and lift coefficients, C_D and C_L, for a circular cylinder placed near a fixed ground in a wind tunnel at Re = $2.0x10^4$, and showed that C_D rapidly decreased and C_L increased as the cylinder comes close to the ground.

Zdravkovich (2003) reported the drag behavior for a cylinder placed near a moving ground running at the same speed as the freestream (i.e., there was practically no boundary layer on the ground) for a higher Reynolds number of $2.5x10^5$. In contrast to the other studies [e.g. Roshko *et al.* (1975), Bearman and Zdravkovich (1978), Angrilli *et al.* (1982), Price *et al.* (2002) and Lin *et al.* (2005)], the decreased in drag due to the decrease in h/d did not occurred in his measurements. It was not clear, however, whether this was attributed to the non-existence of the ground boundary layer or the higher Reynolds number.

Nishino (2007) reproduced the same tests made by Zdravkovich (2003) for Re = $4.0x10^4$ and Re = $1.0x10^5$. The end conditions were taking into account using end-plates. For the case where the end-plates were not used (essentially three-dimensional flow), the C_D curve increased as h/d decreased; it was reported by Nishino (2007) that this behavior occurred due to the no development of a boundary layer on the ground.

Moura (2007) studied numerically the two-dimensional, incompressible unsteady flow around a circular cylinder near a fixed ground using the vortex method. The body was animate by a forced frequency. He investigated the

influence of the heave movement with small amplitude on the aerodynamic loads of the cylinder placed near a fixed ground.

In a recent work, Bimbato (2008) used the vortex method to study the aerodynamic loads acting on a circular cylinder surface placed near a ground running at the same speed as the incident flow in which the vorticity was generate only from the body surface. The results agree with that presented by Nishino (2007) when the end-plates were used.

In this paper, it was used the vortex method to simulate the viscous flow around a circular cylinder in ground effect. Two plane wall configurations are considered: fixed ground and moving ground. In all the numerical experiments the Reynolds number is kept in high value, Re=1.0x10^5. Even with such a high Reynolds number value, no attempt for turbulence modeling were made once these aspects have a strong three-dimensional component; see Alcântara Pereira *et al.* (2002). The numerical results include the time evolution of the lift and drag coefficients as well the instantaneous pressure distributions for strategic chosen instants of the time simulation. These instants of the time were chosen to illustrate the near field wake which is important to understand the flow behavior.

Vortex method offers a number of advantages over the more traditional Eulerian schemes for the analysis of the external flow that develops in a large domain; the main reasons are [Leonard (1980), Sarpkaya (1989), Lewis (1999), Kamemoto (2004), Stock (2007) and Hirata *et al.*, (2008)]: (i) as a fully mesh-less scheme, no grid is necessary; (ii) the computational efforts are directed only to the regions with non-zero vorticity and not to all the domain points as is done in the Eulerian formulations; (iii) the far away downstream boundary condition is taken care automatically which is relevant for the simulation of the flow around a bluff body (or an oscillating body) that has a wide viscous wake.

2. MATHEMATICAL FORMULATION

Consider the viscous flow around a circular cylinder near a fixed plane boundary as shown in Fig. 1. The uniform flow is represented by U and assumed from left to right. The fluid domain Ω is identified by the boundary $S=S_1 \cup S_2 \cup S_3$, S_1 being the body surface, S_2 the plane surface and S_3 the far away boundary.
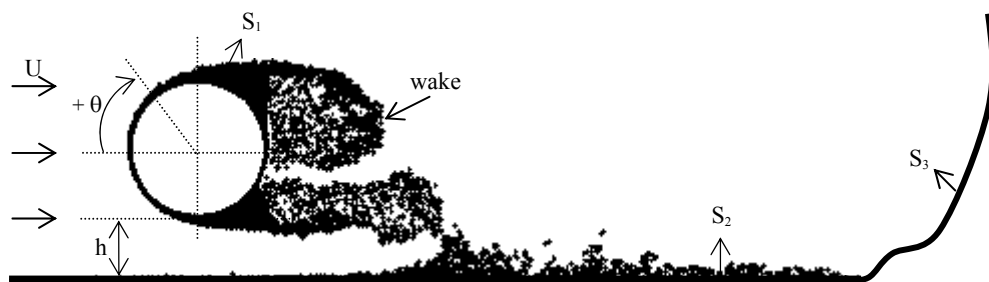

Figure 1. Definitions of the physical domain

The vorticity that develops in the body boundary layer is carried out downstream into the viscous wake. Due to the no-slip condition, a shear flow is set on the fixed ground. As consequence, there is vorticity generated on the fixed ground and the body wake will be influenced by the presence of the plane wall wake, as can be seen in Fig. 1. A ground running at the same speed as the freestream, however, does not allow the development of boundary layer.

For an incompressible flow the continuity equation is written as

$$\nabla \cdot \mathbf{u} = 0 \tag{1}$$

where $\mathbf{u} \equiv (u, v)$ is the velocity vector field.

If, in addition, the fluid is Newtonian with constant properties, the momentum equation is represented by the Navier-Stokes equations as

$$\frac{\partial \mathbf{u}}{\partial t} + \mathbf{u} \cdot \nabla \mathbf{u} = -\frac{1}{\rho} \nabla p + \frac{\mu}{\rho} \nabla^2 \mathbf{u} \tag{2}$$

where p is the pressure, ρ is the density of the fluid and μ is the dynamic viscosity of the fluid.

The impermeability condition on the cylinder and ground surfaces is given by

$$u_n - v_n = 0, \text{ on } S_1 \text{ and } S_2. \tag{3}$$

The no-slip condition is imposed on the cylinder surface and only on the fixed ground; thus

$$u_\tau - v_\tau = 0, \text{ on } S_1 \text{ and } S_2 \quad \text{(for the fixed ground case)} \tag{4a}$$

$u_\tau - v_\tau = 0$, only on S_1 (for the moving ground case). (4b)

Here, it is worth to mention the necessity of imposing the impermeability condition on the surface of the moving ground.

In the three equations above, u_n and u_τ are, respectively, the fluid normal and tangential velocities and v_n and v_τ are, respectively, the solid boundary normal and tangential velocities. One assumes that, far away, the perturbation caused by the body and the plane wall fades as

$$|\mathbf{u}| \rightarrow U \text{ on } S_3 .$$ (5)

3. NUMERICAL METHOD: THE VORTEX METHOD

Important features of the vortex method are: (i) it is a numerical technique suitable for the solution of convection/diffusion type equations like the Navier-Stokes ones; (ii) it is a suitable technique for direct simulation and large-eddy simulation; (iii) it is a mesh free technique; the vorticity field is represented by a cloud of discrete free vortices that move with the fluid velocity.

Taking the curl of Eq. (2) and with some algebraic manipulations one gets the vorticity equation which presents no pressure term. In two-dimensions this equation is written as

$$\frac{\partial \omega}{\partial t} + \mathbf{u} \cdot \nabla \omega = \frac{1}{Re} \nabla^2 \omega .$$ (6)

In the equation above $Re = \dfrac{U d}{\upsilon}$ is the Reynolds number based on the cylinder diameter d and υ is the fluid kinematic viscosity. All the quantities in Eq. (6) and equations bellow are nondimensionalized by U and d.

The left hand side of the Eq. (6) carries all the information needed for the convection of vorticity while the right hand side governs the diffusion of vorticity. The solution to the problem above is obtained using the discrete vortex method. Following Chorin (1973), and based on Eq. (6), it was used an algorithm that splits the convective-diffusive operator in the form

$$\frac{D\omega}{Dt} = \frac{\partial \omega}{\partial t} + (\mathbf{u} \cdot \nabla)\omega = 0$$ (7)

$$\frac{\partial \omega}{\partial t} = \frac{1}{Re} \nabla^2 \omega .$$ (8)

To solve convection of vorticity, governed by Eq. (7), is necessary to calculate the components of the velocity induced at the location of the vortex (j), which ones suffer the influence of three parcels: the incident flow contribution, $\mathbf{ui}(\mathbf{x}, t)$, the solid surfaces contribution, $\mathbf{ub}(\mathbf{x}, t)$ and the vortex cloud contribution, $\mathbf{uv}(\mathbf{x}, t)$. So

$$\mathbf{u}(\mathbf{x}, t) = \mathbf{ui}(\mathbf{x}, t) + \mathbf{ub}(\mathbf{x}, t) + \mathbf{uv}(\mathbf{x}, t) \text{ at vortex (j).}$$ (9)

The incident flow contribution is given by

$$ui_1 = 1 \quad \text{and} \quad ui_2 = 0 .$$ (10)

The solid surfaces contribution is obtained by the Panels Method (Katz and Plotkin, 1991); thus

$$ub_i(x_j, t) = \sum_{k=1}^{NP} \psi_k c_{jk}^i (x_j(t) - x_k) , \text{ i=1, 2 and j=1, Z}$$ (11)

where Z is the total number of discrete vortices on the cloud, and NP is the number of sources flat panels used to represent the body and the ground surfaces. It is assumed that the source strength per length is constant such that ψ_k=const and $c_{jk}^i(x_j(t) - x_k)$ is the i-component of the velocity induced at a discrete vortex (j) by a source panel k.

Finally, the contribution of the vortex cloud is

$$uv_i\left(x_j,t\right)=\sum_{k=1}^{Z}\Gamma_k c_{jk}^i\left(x_j(t)-x_k\right) , \; i=1,2 \tag{12}$$

where Γ_k is k-vortex intensity and $c_{jk}^i\left(x_j(t)-x_k\right)$ is the i-component of the velocity induced at a discrete vortex (j) by a k-vortex with unit intensity.

In this work, one uses the Lamb vortex model (Mustto *et al.*, 1998)

$$u_{\theta jk}=-\frac{\Gamma_k}{2\pi}\frac{1}{r_{jk}}\left[1-\exp\left(-5.02572\frac{r_{jk}^2}{\sigma_0^2}\right)\right] \tag{13}$$

where $u_{\theta jk}$ is the circumferential velocity induced on the vortex (j) by a vortex located at k, r_{jk} is the distance between the two vortices and σ_0 is the Lamb vortex core of the k-vortex.

With the three parcels calculated previously, Eq. (7) can be solved by the first order Euler scheme

$$x_j\left(t+\Delta t\right)=x_j(t)+u_j(\mathbf{x},t)\Delta t \; , \; j=1, Z \tag{14a}$$

$$y_j\left(t+\Delta t\right)=y_j(t)+v_j(\mathbf{y},t)\Delta t \; , \; j=1, Z \tag{14b}$$

where Δt is the time increment.

Equation (8) is solved by the random walk method (Lewis, 1999); the random displacement with a zero mean and a $(2\Delta t/Re)$ variance, for the vortex (j) is defined as

$$\chi_j\equiv\left(\chi_{1j},\chi_{2j}\right)=\sqrt{\frac{4\Delta t}{Re}\ln\left(\frac{1}{P}\right)}\left[\cos(2\pi Q)+i\operatorname{sen}(2\pi Q)\right] \tag{15}$$

where $i=\sqrt{-1}$, P and Q are random numbers between 0.0 and 1.0.

Once, with the vorticity field the pressure calculation starts with the Bernoulli function, defined by Uhlman (1992) as

$$\overline{Y}=p+\frac{u^2}{2}, \; u=\left|\mathbf{u}\right| . \tag{16}$$

Kamemoto (1993) used the same function and starting from the Navier-Stokes equations was able to write a Poisson equation for the pressure. This equation was solved using a finite difference scheme. Here the same Poisson equation was derived and its solution was obtained through the following integral formulation (Shintani and Akamatsu, 1994)

$$H\overline{Y_i}-\int_S\overline{Y}\nabla\Xi_i\cdot\mathbf{e}_n dS=\iint_\Omega\nabla\Xi_i\cdot(\mathbf{u}\times\boldsymbol{\omega})d\Omega-\frac{1}{Re}\int_S(\nabla\Xi_i\times\boldsymbol{\omega})\cdot\mathbf{e}_n dS \tag{17}$$

where $H=1$ in the fluid domain, $H=0.5$ on the boundaries, Ξ is a fundamental solution of the Laplace equation and $\mathbf{e}_n$ is the unit vector normal to the solid surfaces.

The drag and lift coefficients are expressed by

$$C_D=-\sum_{k=1}^{NP}2(p_k-p_\infty)\Delta S_k\sin\beta_k=-\sum_{k=1}^{NP}C_P\Delta S_k\sin\beta_k \tag{18}$$

$$C_L=-\sum_{k=1}^{NP}2(p_k-p_\infty)\Delta S_k\cos\beta_k=-\sum_{k=1}^{NP}C_P\Delta S_k\cos\beta_k \tag{19}$$

where ΔS_k is the length and β_k is the angle and both of the k-panel.

4. NUMERICAL SIMULATION OF THE FLOW AROUND A CIRCULAR CYLINDER

4.1. Isolated Circular Cylinder

First, it was investigated the flow around an isolated circular cylinder to analyze the consistence of the vortex code and to define some numerical parameters, as for example the number of panels used to define the cylinder surface. For this particular configuration, each cylinder and ground surfaces were represented by MB=300 flat source panels with constant density. The simulation was performed up to 1000 time steps with magnitude Δt=0.05. During each time step the new vortex elements are shedding into the cloud through a displacement ε=σ₀=0.001d normal to the straight-line elements (panels); see Ricci (2002).

Table 1 shows that the numerical results agree very well with the experimental ones obtained by Blevins (1984), which have an uncertainty of about 10%. The results from Mustto *et al*. (1998) were obtained numerically using a slightly different vortex method from the present implementation. The agreement between the two numerical methods is very good for the Strouhal number, and both results are close to the experimental value. The present drag coefficient shows a higher value as compared to the experimental result. One should observe, that the three-dimensional effects are non-negligible for the Reynolds number used in the present simulation (Re = 1.0×10^5). Therefore it can be expected that a two-dimensional computation of such flow must produce higher values for the drag coefficient. On the other hand, the Strouhal number is insensitive to these three-dimensional effects. The mean numerical lift coefficient, although very small, is not zero which is due to numerical approximations. The aerodynamic forces computations were evaluated between t=30 and t=50.

Table 1. Mean values of drag and lift coefficients and Strouhal number of an isolated circular cylinder

$Re = 1.0 \times 10^5$	$\overline{C_D}$	$\overline{C_L}$	$\overline{St}$
Blevins (1984)	1.20	-	0.19
Mustto *et al*. (1998)	1.22	-	0.22
Present Simulation	1.25	0.02	0.19

The Strouhal number is defined as

$$St = \frac{f\,d}{U} \tag{20}$$

where f is the detachment frequency of vortices.

More details of this preliminary study are discussed in Bimbato (2008) and Bimbato *et al*. (2008).

4.2. Circular Cylinder in Ground Effect
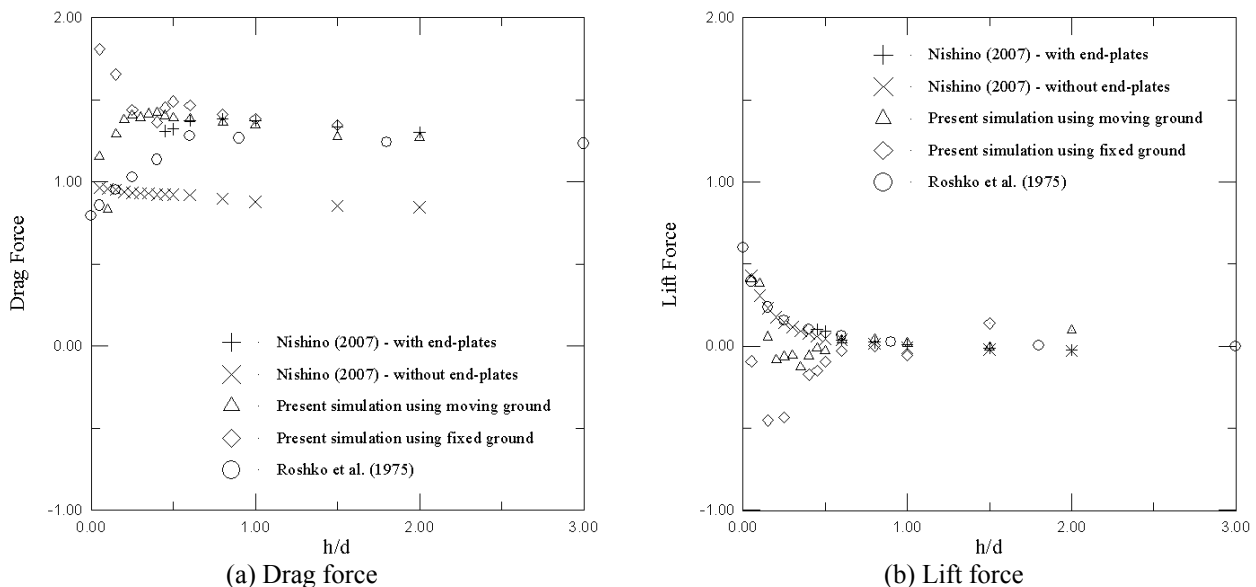

(a) Drag force (b) Lift force

Figure 2. Time-averaged drag and lift coefficients *vs*. gap ratio for different end conditions

Figure 2 shows the behavior of drag and lift coefficients for circular cylinder at different values of the gap-ratio h/d and for different end conditions. The present numerical results are referred as "moving ground" and as "fixed ground" in Fig. 2. Columns 5 and 6 of Table 2 presents the numerical values for drag coefficient.

Nishino (2007) investigated two flow configurations: one was essentially three-dimensional and another approximately two-dimensional; this second configuration was obtained by using end-plates on the cylinder extremity. It was shown that the drag coefficient on the 3-D flow increased slightly as the cylinder comes close to the ground, while the 2-D flow presented a higher drag coefficient.

The present simulations using moving ground reproduce the situation studied by Nishino (2007) with end-plates. In Fig. 2a is shown that the drag coefficient results of the 2-D numerical simulation agree well with the experimental results approximately 2-D from Nishino (2007). It is worth to observe that in this situation, due to the experimental difficulties, he was not able to perform the tests for small-gap regime (h/d<0.45).

On the same plot is shown the present results, obtained with fixed ground to simulate the influence of the boundary layer that develops on the ground and interferes with the body viscous wake. In this case, the drag coefficient agrees well with the experiments reported by Roshko *et al.* (1975) for higher gap-ratios.

In Fig. 2b is shown that the numerical lift coefficient curves follows quite well the values obtained experimentally, except when 0.2<h/d<0.5 where the computed values are smaller. For smaller values of the gap-ratio there are no experimental values available when the end-plates are added to the cylinder. However, it is worth to observe that all the experimental and numerical results indicate the same limiting value for really small gap-ratio.

Table 2. Summary of results for drag coefficient on the flow around circular cylinder near a plane boundary

h/d	Nishino (2007) without end-plates	Nishino (2007) with end-plates	Roshko *et al.* (1975)	Present simulation using moving ground	Present simulation using fixed ground
0.00	-	-	0.795	-	-
0.05	0.965	-	0.857	1.154	1.809
0.10	0.958	-	-	0.832	-
0.15	0.952	-	0.954	1.293	1.656
0.20	0.939	-	-	1.376	-
0.25	0.933	-	1.029	1.406	1.440
0.30	0.930	-	-	1.393	-
0.35	0.931	-	-	1.415	-
0.40	0.922	-	1.136	1.421	1.365
0.45	0.926	1.311	-	1.403	1.453
0.50	0.924	1.323	-	1.391	1.491
0.60	0.920	1.373	1.281	1.383	1.466
0.80	0.899	1.385	-	1.362	1.410
0.90	-	-	1.266	-	-
1.00	0.881	1.375	-	1.346	1.385
1.50	0.854	1.337	-	1.277	1.346
1.80	-	-	1.243	-	-
2.00	0.845	1.304	-	1.269	-
3.00	-	-	1.234	-	-

The following analysis for the mechanisms of the wake interference on the aerodynamic loads behavior is based on the gap-ratio h/d=0.45; see Tab. 2.
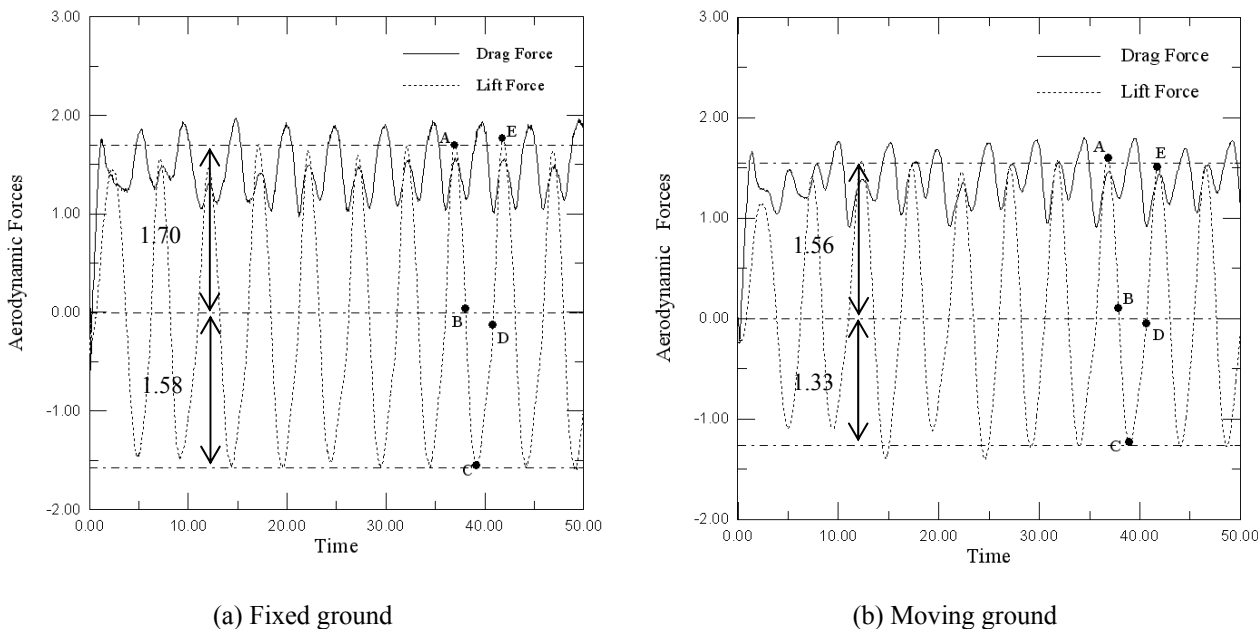
Figure 3 shows the time evolution of the aerodynamic forces acting on the circular cylinder surface placed near a fixed ground (see Fig. 3a) and near a moving ground (see Fig. 3b). Due to the proximity of the ground the C_D curves present a pair of small extreme values (small departure of the maximum and minimum values from the mean drag value) followed by a pair of large extreme value (large departure of the maximum and minimum values from the mean drag value). The fluctuation of C_D has twice the frequency that the C_L, because it fluctuates once for each upper and lower shedding.

The absolute values of the maximum of C_L curves are also presented in Fig. 3. When the ground is fixed, it can be observed that the C_L curve has higher absolute value of the maximum than the absolute value of the maximum of the moving ground C_L curve case.

Figure 4 shows plots of instantaneous pressure distributions on the cylinder surface. Distributions A, B, C, D and E are related to instants A, B, C, D and E as indicated in Fig. 3. It can be seen in Fig. 4 differences between the instantaneous pressure distributions on the cylinder surface using fixed ground and moving ground.

At instant represented by the point A in Fig. 4a and Fig. 4b, it was observed a low pressure zone on the upper side of the cylinder surface, which explains the maximum C_L value; see Fig. 3a and Fig. 3b. At this moment a clockwise vortex structure is detaching from the upper surface; see Fig. 5a and Fig. 5b.

Instant B is defined in Fig. 4 as the moment in which appears an approximately constant pressure zone; this moment explains the null value for C_L curve and the minimum value for C_D curve. The structure that was born at instant A starts growing as an equivalent physical description of the mechanism of the vortex-formation region described by Gerrard (1966); see Fig. 6.
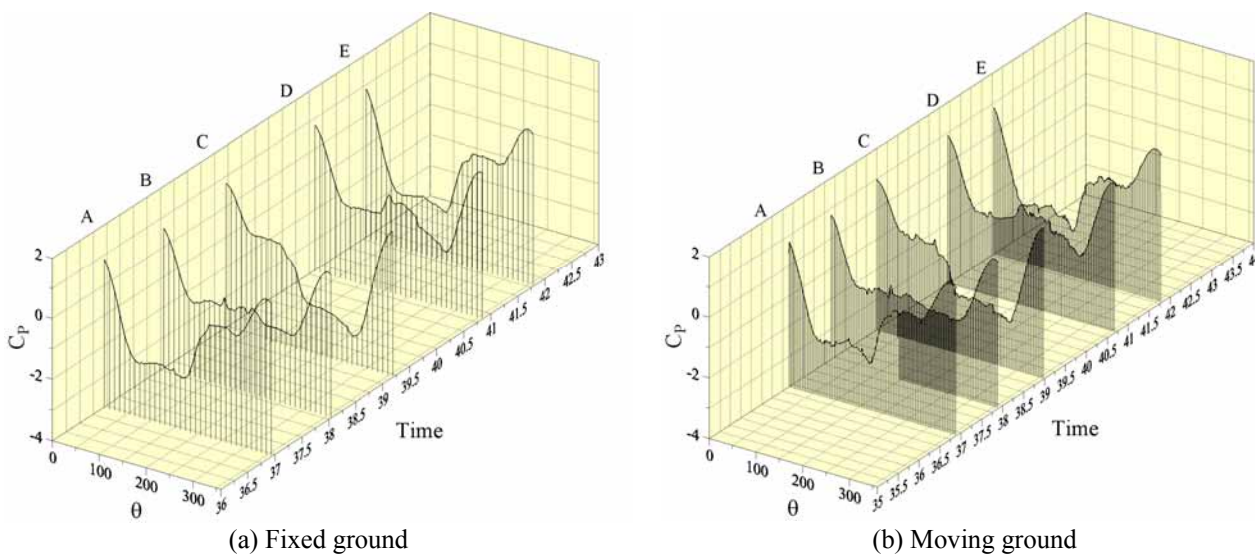

(a) Fixed ground
(b) Moving ground

Figure 3. Time evolution of the aerodynamic loads; Re=1.0x10^5 and h/d=0.45

Around an instant represented by point C of Fig. 4, it can be seen a low pressure zone on the lower side of the cylinder surface, which explains the minimum C_L; see Fig. 3. At this moment a counter-clockwise structure is detaching from the lower side of the cylinder surface; see Fig. 7. Simultaneously, the clockwise structure that was born at instant A and growed around the instant B starts to be incorporate to the body wake; in this moment the C_D coefficient has a maximum value.

(a) Fixed ground
(b) Moving ground

Figure 4. Instantaneous pressure distribution for the circular cylinder in ground effect, Re=1.0x10^5 and h/d=0.45

The same sequence of events repeats all over again. The alternate amplitudes of C_D curve (greater and smaller) occurs due to the vortex structure that started at instant A and can grow with freedom until be incorporated by the body

wake around instant C (maximum C_D corresponds to the greater amplitude). On the other hand, the vortex structure that started at the lower side of the cylinder surface at instant C can not grow with freedom; this structure is limited by the ground plane in a manner that when it is incorporated by the body wake around instant E or A (these instants are equivalent), C_D can not achieve the same value of the previous period – one tells that C_D achieves a smaller maximum value. To visualize the limitation on the growth of the counter-clockwise vortex structure, compare Fig. 5 and Fig. 7.
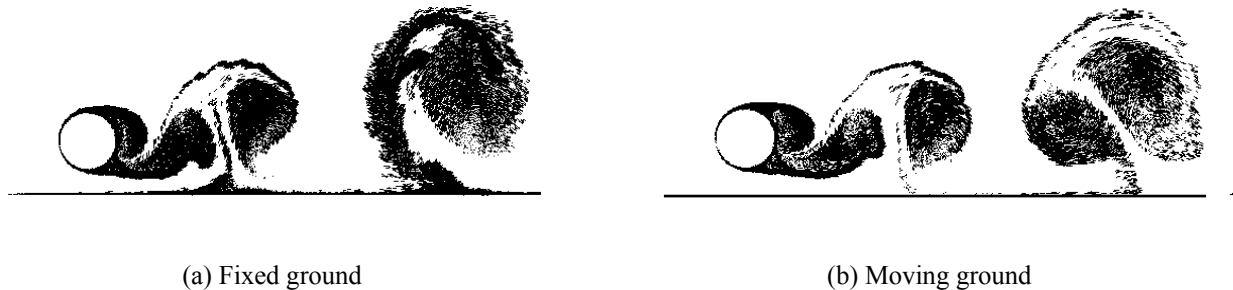

(a) Fixed ground   (b) Moving ground

Figure 5. Near field velocity distribution at an instant represented by point A; Re=1.0x10^5 and h/d=0.45

From which was exposed, it can be concluded that the wake interference mechanism has a significance influence on the aerodynamic loads behavior acting on the circular cylinder. When this effect is present (Fig. 5a, Fig. 6a, Fig. 7a and Fig. 8a) is identified that the wake from the ground interferes in the body wake. This comportment causes a higher drag than the case when the wake interference effect is not present (Fig. 5b, Fig. 6b, Fig. 7b and Fig. 8b).

(a) Fixed ground   (b) Moving ground

Figure 6. Near field velocity distribution at an instant represented by point B; Re=1.0x10^5 and h/d=0.45

Besides that, the present results using fixed ground show that the absolute value of the maximum of C_L curve is bigger than the one obtained by the moving ground. However, this fact not means that the net C_L is higher, which has a practical importance. As soon in Fig. 3, as the numerical transient is over and a periodic regimes reached (from t = 15 on, approximately) the lift coefficient oscillates between -1.58 and 1.70, approximately, to the fixed ground case and oscillates between -1.33 and 1.56, approximately, to the moving ground case.

(a) Fixed ground   (b) Moving ground

Figure 7. Near field velocity distribution at an instant represented by point C; Re=1.0x10^5 and h/d=0.45

According to Nishino (2007), see also Tab. 2, there are three gap regimes on the flow around circular cylinders near a plane boundary: large-gap (h/d > 0.50), intermediate-gap (0.35 < h/d < 0.50), and small-gap (h/d < 0.35) regimes.

Figure 9 shows the position of the wake vortices for the gap-ratio h/d →∞ at the last step of the computation (t=50) where the formation and shedding of large eddies in the wake is very clear. It can also been visualized the vortex pairing process, where the vortices rotate in opposite directions and are connected to each other by a vortex sheet. The

rightmost part of the wake corresponds to the numerical transient that occurs before a periodic steady state regime is reached.
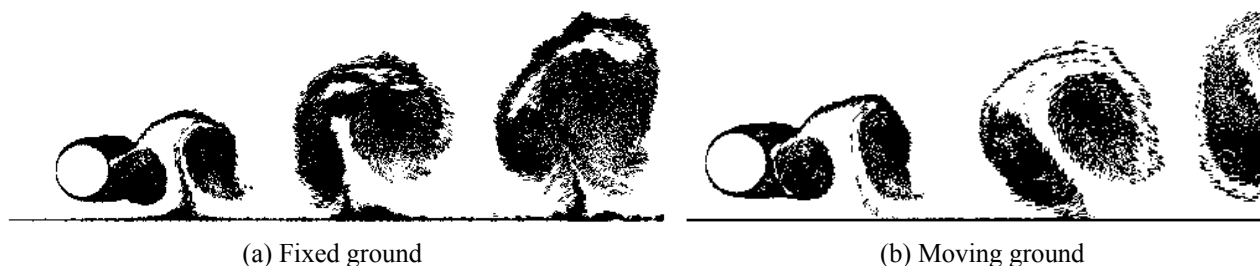

(a) Fixed ground   (b) Moving ground

Figure 8. Near field velocity distribution at an instant represented by point D; Re=1.0×10^5 and h/d=0.45

For a not so small gap, see Fig. 5, Fig. 6, Fig. 7 and Fig. 8, the wake seems to be formed by a series of "mushroom" type of vortex structures, which will be destroyed far away by the ground effect.

Further analyses are necessary to understand the aerodynamic loads and vortex shedding behavior when the body is brought close to the plane wall.

Figure 9. Position of the wake vortices at t=50 for an isolated cylinder case; Re=1.0×10^5 and h/d$\rightarrow\infty$.

5. CONCLUSIONS

The present simulations show a Lagrangian-type numerical scheme capable of solving unsteady separated flows in the vicinity of a plane wall with a high value of the Reynolds number. The methodology developed in this paper to understand the complex mechanisms of ground effect is greatly simplified by the utilization of the vortex method.

Two models of plane wall are considered: with and without moving ground. The results are able to predict the main features of the flow around a body (although with a simple geometrical shape) in ground effect. When using fixed ground, the absolute value of the maximum of the C_D curve is bigger than the absolute value of the maximum of the moving ground C_D curve; the wake interference is the one responsible for a "great" maximum value of the C_D curve.

The instantaneous pressure distribution on the cylinder surface allows one to follows, in time, its evolution. This feature can be of importance when the body is oscillating near a ground plane and in many other situations of practical interest. It becomes obvious that one have a powerful tool if the time evolution of the pressure distribution is analyzed simultaneously with the integrated loads (lift and drag).

The experience gained with the present work allows the authors to analyze complex situations where relative motions between bodies are present. These extend the applicability of the numerical code.

Finally, despite the differences presented, the results are promising, which encourages performing additional tests in order to explore the phenomena in more details.

6. ACKNOWLEDGEMENTS

7. REFERENCES

Alcântara Pereira, L. A., Ricci, J. E. R., Hirata, M. H. and Silveira Neto, A., 2002, "Simulation of Vortex-Shedding Flow about a Circular Cylinder with Turbulence Modeling", International Society of CFD, Vol. 11, No. 3, October, pp. 315-322.

Angrilli, F., Bergamaschi, S. and Cossalter, V., 1982, "Investigation of Wall Induced Modifications to Vortex Shedding from a Circular Cylinder", Transactions of the ASME: Journal of Fluids Engineering, Vol. 104, pp. 518-522.

Bearman, P. W. and Zdravkovich, M. M., 1978, "Flow around a Circular Cylinder near a Plane Boundary", Journal of Fluid Mechanics, Vol. 89, pp. 33-47.

Bimbato, A. M., 2008, Analysis of Moving Ground Effects on the Aerodynamic Loads of a Body, M.Sc. Dissertation, IEM/UNIFEI (in Portuguese).

Bimbato, A. M., Alcântara Pereira, L. A. and Hirata, M. H., 2008, "Analysis of the Aerodynamics Loads in a Circular Cylinder near a Moving Ground", 12th Brazilian Congress of Thermal Sciences and Engineering, November, 10-14, Belo Horizonte, MG, Brazil.

Blevins, R. D., 1984, Applied Fluid Dynamics Handbook, Van Nostrand Reinhold, Co.

Chorin, A. J., 1973, "Numerical Study of Slightly Viscous Flow", Journal of Fluid Mechanics, Vol. 57, pp. 785-796.

Gerrard, J. H., 1966, "The Mechanics of the Formation Region of Vortices behind Bluff Bodies", J. Fluid Mech., 25: 401-413.

Hirata, M. H., Alcântara Pereira, L. A., Recicar, J. N., Moura, W. H., 2008, "High Reynolds Number Oscillations of a Circular Cylinder", J. of the Braz. Soc. Of Mech. Sci. & Eng., Vol. XXX, No. 4, pp. 300-308.

Kamemoto, K., 1993, "Procedure to Estimate Unstead Pressure Distribution for Vortex Method" (In Japanese), Trans. Jpn. Soc. Mech. Eng., Vol. 59, No. 568 B, pp. 3708-3713.

Kamemoto, K., 2004, "On Contribution of Advanced Vortex Element Methods Toward Virtual Reality of Unsteady Vortical Flows in the New Generation of CFD", Proceedings of the 10th Brazilian Congress of Thermal Sciences and Engineering-ENCIT 2004, Rio de Janeiro, Brazil, Nov. 29 - Dec. 03, Invited Lecture-CIT04-IL04.

Katz, J. and Plotkin, A., 1991, "Low Speed Aerodynamics: From Wing Theory to Panel Methods", McGraw Hill, Inc.

Leonard, A., 1980, "Vortex Methods for Flow Simulation", J. Comput. Phys., Vol. 37, pp. 289-335.

Lewis, R. I., 1999, "Vortex Element Methods, the Most Natural Approach to Flow Simulation - A Review of Methodology with Applications", Proceedings of 1st Int. Conference on Vortex Methods, Kobe, Nov. 4-5, pp. 1-15.

Lin, C., Lin, W. J. and Lin, S. S., 2005, "Flow Characteristics around a Circular Cylinder near a Plane Boundary", Proceedings of the Sixteenth International Symposium on Transport Phenomena (ISTP-16), 29 August – 1 September, Prague, Czech Republic, (CD-ROOM).

Moura, W. H., 2007, Analysis of the Flow around an Oscillating Circular Cylinder in the Vicinity of a Ground Plane, M.Sc. Dissertation, IEM/UNIFEI (in Portuguese).

Mustto, A. A., Hirata, M. H. and Bodstein, G. C. R., 1998, "Discrete Vortex Method Simulation of the Flow Around a Circular Cylinder with and without Rotation", A.I.A.A. Paper 98-2409, Proceedings of the 16th A.I.A.A. Applied Aerodynamics Conference, Albuquerque, NM, USA, June.

Nishino, T., 2007, Dynamics and Stability of Flow Past a Circular Cylinder in Ground Effect, Ph.D. Thesis, Faculty of Engineering, Science and Mathematics, University of Southampton, 145p.

Price, S. J., Summer, D., Smith, J. G., Leong, K. and Paidoussis, M. P., 2002, "Flow Vizualization around a Circular Cylinder near to a Plane Wall", Journal of Fluids and Structures, Vol. 16, pp. 175-191.

Ricci, J. E. R., 2002, "Numerical Simulation of the Flow around a Body in the Vicinity of a Plane Using Vortex Method", Ph.D. Thesis, Mechanical Engineering Institute, UNIFEI, Itajubá, MG, Brazil (in Portuguese).

Roshko, A., Steinolfson, A. and Chattoorgoon, V., 1975, "Flow Forces on a Cylinder near a Wall or near another Cylinder", Proceedings of the 2nd U.S. National Conference on Wind Engineering Research, Fort Collins, Paper IV-15.

Sarpkaya, T., 1989, "Computational Methods with Vortices - The 1988 Freeman Scholar Lecture", Journal of Fluids Engineering, Vol. 111, pp. 5-52.

Shintani, M. and Akamatsu, T., 1994, "Investigation of Two Dimensional Discrete Vortex Method with Viscous Diffusion Model", Computational Fluid Dynamics Journal, Vol. 3, No. 2, pp. 237-254.

Stock, M. J., 2007, "Summary of Vortex Methods Literature (A lifting document rife with opinion)", April, 18: © 2002-2007 Mark J. Stock.

Uhlman, J. S., 1992, "An Integral Equation Formulation of the Equation of an Incompressible Fluid", Naval Undersea Warfare Center, T.R. 10-086.

Zdravkovich, M. M., 2003, Flow around Circular Cylinders: Vol. 2: Applications, Oxford University Press, Oxford, UK.

8. RESPONSIBILITY NOTICE

The authors are the only responsibles for the printed material included in this paper.